NKX3.1 Activates Expression of Insulin-like Growth Factor Binding Protein-3 to Mediate Insulin-like Growth Factor-I Signaling and Cell Proliferation

Erin Muhlbradt,[1] Ekaterina Asatiani,[1] Elizabeth Ortner,[1] Antai Wang,[1] and Edward P. Gelmann[1,2]

[1]Lombardi Comprehensive Cancer Center, Washington, District of Columbia and [2]Departments of Medicine and Pathology, Herbert Irving Comprehensive Cancer Center, Columbia University, New York, New York

Abstract

NKX3.1 is a homeobox gene that codes for a haploinsufficient prostate cancer tumor suppressor. NKX3.1 protein levels are down-regulated in the majority of primary prostate cancer tissues. NKX3.1 expression in PC-3 cells increased insulin-like growth factor binding protein-3 (IGFBP-3) mRNA expression 10-fold as determined by expression microarray analysis. In both stably and transiently transfected PC-3 cells and in LNCaP cells, NKX3.1 expression increased IGFBP-3 mRNA and protein expression. In prostates of *Nkx3.1* gene-targeted mice *Igfbp-3* mRNA levels correlated with *Nkx3.1* copy number. NKX3.1 expression in PC-3 cells attenuated the ability of insulin-like growth factor-I (IGF-I) to induce phosphorylation of type I IGF receptor (IGF-IR), insulin receptor substrate 1, phosphatidylinositol 3-kinase, and AKT. The effect of NKX3.1 on IGF-I signaling was not seen when cells were exposed to long-R3-IGF-I, an IGF-I variant peptide that does not bind to IGFBP-3. Additionally, small interfering RNA–induced knockdown of IGFBP-3 expression partially reversed the attenuation of IGF-IR signaling by NKX3.1 and abrogated NKX3.1 suppression of PC-3 cell proliferation. Thus, there is a close relationship *in vitro* and *in vivo* between NKX3.1 and IGFBP-3. The growth-suppressive effects of NKX3.1 in prostate cells are mediated, in part, by activation of IGFBP-3 expression. [Cancer Res 2009;69(6):2615–22]

Introduction

Adenocarcinoma of the prostate, like many epithelial malignancies, initiates in luminal epithelial cells in prostatic ducts that acquire the precursor or gatekeeper mutations required for development of the malignant phenotype. Early in prostate cancer, a region of 8p21.2 is lost in the majority of cancers (1). At least one target for 8p21.2 loss is the homeobox gene *NKX3.1*, which is expressed specifically in prostate luminal epithelial cells. NKX3.1 undergoes progressive loss of protein expression during prostate cancer progression from hormone dependence to hormone independence and metastatic disease (2, 3).

The *Nkx3.1* gene is not subject to somatic mutation in prostate cancer (4, 5). Gene targeting studies in mice showed that NKX3.1 haploinsufficiency alone can predispose to prostate epithelial dysplasia and can cooperate with other oncogenic mutations to augment prostate carcinogenesis (6, 7). In gene-targeted mice,

decreased Nkx3.1 expression is accompanied by decreased expression of genes under the regulation of the Nkx3.l homeoprotein (8). We have recently shown that diminished levels of NKX3.1 expression in primary human prostate cancer and intraepithelial neoplasia correlated with the degree of gene inactivation by deletion, methylation, or both. Not only is NKX3.1 down-regulated in preinvasive prostate cancer but NKX3.1 expression is also reduced in regions of inflammatory atrophy that are precursors for malignant transformation (9). Inflammatory cytokines in these lesions can induce ubiquitination of NKX3.1 and protein loss (10). Therefore, NKX3.1 may play a role in premalignant events in the prostate gland by modulating gene expression to increase the susceptibility of prostate epithelial cells to malignant transformation. We have sought to characterize the gene expression program activated by NKX3.1 in human cells. Here we show *in vitro* and *in vivo* that NKX3.1 activates expression of insulin-like growth factor binding protein-3 (IGFBP-3), a known growth suppressor protein and down-regulator of insulin-like growth factor-I (IGF-I) activity.

IGFBP-3 is one of six IGFBPs that bind to and modulate the activity of IGFs. IGFBP-3 is a highly abundant serum protein and therefore affects the physiologic bioavailability of circulating IGF-I (11). In the pericellular environment, IGFBP-3 is thought to be proapoptotic and to counteract the proliferative effects of IGF-I (12). Pericellular proteases cleave IGFBP-3, thus releasing IGF-I to bind to the type I IGF receptor (IGF-IR). For example, prostate-specific antigen is a metalloproteinase that cleaves IGFBP-3 to yield at least seven proteolytic fragments, some of which retain the ability to bind IGF-I, albeit with lower affinity than the intact protein (13–16). The interaction of IGFBP-3 with cells is more complex than suggested by its interactions with IGF-I. IGFBP-3 stimulates cells directly as shown by the biological effects of IGFBP-3 mutant proteins that lack IGF-I binding (17). Interestingly, although IGFBP-3 expression was not identified in a high-throughput expression analysis of *Nkx3.1* gene-targeted mice (8), IGFBP-3 was identified as a major target of down-regulation in prostate cancer compared with nonmalignant prostate tissue (18). We now present data showing a role for IGFBP-3 in growth suppression by NKX3.1. We propose that IGFBP-3 expression represents an important mechanistic link between the tumor-suppressive effects of NKX3.1 and the prosurvival and proliferative effects of IGF-I, a peptide growth factor that has been implicated in prostate carcinogenesis.

Materials and Methods

Expression array analysis. Total RNA from stable PC-3(NKX3.1) and PC-3(pcDNA3.1) cells was harvested using the RNeasy Miniprep kit (Qiagen, Inc.). First-strand cDNA synthesis from total RNA was carried out using the GeneChip T7-Oligo(dT) primer kit (Affymetrix). Second-strand

cDNA synthesis was done using the SuperScript Choice System (Invitrogen). The cDNA was then processed using the GeneChip Sample Cleanup Module (Affymetrix). Amplification and biotin labeling of antisense cRNA were carried out using the BioArray High Efficiency RNA Transcript Labeling system (Affymetrix). Finally, the GeneChip Sample Cleanup Module (Affymetrix) was used to clean up the biotinylated cRNA before it was sent for analysis on an Affymetrix U-133 array system.

Cell culture and reagents. The prostate cancer cell lines PC-3 and LNCaP and the A172 human glioblastoma cell line were obtained from American Type Culture Collection. PC-3 and A172 cell lines were grown in modified IMEM (Invitrogen) containing 10% fetal bovine serum (FBS). LNCaP cells were grown in modified IMEM with phenol red (Invitrogen) containing 10% FBS. The PC-3 cells stably expressing the NKX3.1 expression vector were continuously grown in modified IMEM (Invitrogen) containing 10% FBS and 1.2 mg/mL G418 (Invitrogen). LNCaP cells were serum starved overnight in IMEM supplemented with 5% charcoal-stripped calf serum and treated with 10 nmol/L R1881 for 48 h before harvesting.

Plasmids and transfection. Full-length NKX3.1 was cloned into the mammalian expression vector pcDNA3.1 (Invitrogen) as previously described (19). The phosphatase and tensin homologue (PTEN) expression vector, cloned into pcDNA3.1, was a kind gift from Charles Sawyers (Memorial Sloan-Kettering Cancer Center, New York, NY; ref. 20). Transient and stable transfections were carried out in 75-cm^2 cell culture flasks (Corning, Inc.). Briefly, PC-3 and LNCaP prostate cancer cells were grown to 40% to 60% confluence, and 4 μg of plasmid DNA were transfected into the cell lines using Lipofectamine Plus reagents (Invitrogen) in Opti-MEM (Invitrogen). After a 4-h incubation, the medium was replaced with IMEM containing 10% FBS for an additional 24 h. The PC-3 clones that stably express NKX3.1 were derived by transfection. After 4-h incubation with transfection reagent, PC-3 cells were trypsinized and seeded at a 1:30 density in Falcon Integrid 20 mm grid tissue culture dishes (Becton Dickinson) in modified IMEM containing 10% FBS and 1.2 mg/mL G418 (Invitrogen). The medium was replaced every 4 d until colonies derived from a single cell could be seen with a light microscope. Single-clone colonies were isolated with sterile cloning discs (Scienceware) soaked in 0.25% trypsin-EDTA (Invitrogen) and grown to confluence in six-well tissue culture dishes (Corning) for further study.

Western blot analysis. Cells were grown to 60% to 80% confluence and medium was aspirated from the tissues culture dish. Immediately following medium aspiration, lysis buffer was pipetted directly onto the cell monolayer and cells were scraped from the tissue culture flask. Cells were lysed with radioimmunoprecipitation assay buffer containing Complete Mini protease inhibitors (Roche) and/or phosphatase inhibitors (Cell Signaling) followed by brief sonication to complete lysis. Sixty to ninety micrograms of total cell lysate were boiled in Novex 2× Tris-glycine SDS sample buffer (Invitrogen) containing β-mercaptoethanol for 6 min and resolved on a 10% to 20% Tris-glycine SDS-PAGE gel (Invitrogen). Protein was then transferred onto a nitrocellulose membrane (Bio-Rad) and probed with primary antibodies at the following concentrations: β-actin (Sigma), 1:10,000; NKX3.1 (ref. 2), 1:2,000; IGFBP-3 (Santa Cruz Biotechnology), 1:8,000; AKT (Cell Signaling), 1:7,500; phospho-AKT Thr308 (Cell Signaling), 1:7,500, at 4°C overnight, followed by three washes in PBST. Horseradish peroxidase–conjugated goat anti-rabbit and goat anti-mouse (ImmunoPure antibodies, Pierce Biotechnology) secondary antibodies in 1% milk or 1% bovine serum albumin were applied for 1 h at room temperature. Signal detection was done with SuperSignal West Pico Chemiluminescent Substrate (Pierce Biotechnology).

Reverse transcription-PCR analysis. Total RNA was extracted using the RNeasy Mini Kit (Qiagen) and cells were homogenized using the Qiashredder (Qiagen) method. RNA (125–250 ng) was added to the reverse transcription-PCR (RT-PCR) master mix from OneStep RT-PCR Kit (Qiagen; includes 5× buffer, deoxynucleotide triphosphates, and Taq polymerase). The following primers were used in the RT-PCR reactions: β-actin (fwd 5′-GGCCACGGCTGCTTC-3′ and rev 5′-GTTGGCGTACAGGTCTTTGC-3′), NKX3.1 (fwd 5′-GCCGCACGAGCAGCCAGAGACA-3′ and rev 5′-TTCAGGG-CCGGCAAAGAGGAGTG-3′), IGFBP-3 (fwd 5′-CGCCAGCTCCAGGAAATG-

3′ and rev 5′-GCATGCCCTTTCTTGATGATG-3′), IGFBP-4 (fwd 5′-TTAGCC-CAAGAGGTCTGAGC-3′ and rev 5′-CTGTGCTTCAAGTCTTCCTTTG-3′), and lamin A/C (fwd 5′-AACTTCAGGATGAGATGCTGCG-3′ and rev 5′-GT-CCAGAAGCTCCTGGTACTCGT-3′). RT-PCR was done in a Techne Techgene PCR machine; 30 min at 50°C, 15 min at 94°C, 22 to 30 cycles of 30 s to 1 min at 94°C, 30 s to 1 min at melting temperatures of 55°C to 65°C, and 30 s to 1 min at 72°C, followed by 15 min at 72°C. Samples were stored on ice until and mixed with 10× Blue Juice gel loading buffer (Invitrogen) and run on a 1.5% agarose gel containing 0.1 μg/mL ethidium bromide in Tris-acetate-EDTA buffer. Gels were imaged on a luminometer and recorded using a Kodak one-dimensional digital camera.

Real-time RT-PCR analysis of murine prostate RNA. Frozen anterior prostates from three individual mice of each of genotypes $Nkx3.1^{+/+}$, $Nkx3.1^{+/-}$, and $Nkx3.1^{-/-}$, from both 4- and 12 mo-old animals, were generously provided by Cory Abate-Shen (Columbia University, New York, NY; ref. 6). mRNA was extracted using Qiagen RNeasy mini kit. The real-time quantitative PCR TaqMan assays were done on the ABI PRISM 7700 Sequence Detection System (SDS) equipment (Applied Biosystems). The primers and probe were selected for *igfbp-3* using Primer Express software (Applied Biosystems). The primer sequences were forward, 5′-GCAGG-CAGCCTAAGCACC-3′, and reverse, 5′-CCTCCTCGGACTCACTGAT-3′. The probe sequence (TCCCCTCCCAACCTGCTCCAGG) was labeled at the 5′ end with the reporter molecule 6-carboxyfluorescein (FAM) and at the 3′ with the quencher BHQ-1. Amplification of commercially available endogenous VIC-labeled control, rodent glyceraldehyde-3-phosphate dehydrogenase (GAPDH; Applied Biosystems), was used to standardize the amount of sample DNA added. Dilutions of DNA from the cell line (LNCaP) were used to construct standard curves for the target gene and endogenous control. TaqMan Universal PCR Master Mix was combined with 100 ng of sample DNA, 900 nmol/L final concentration of primers, and 100 nmol/L final concentration of the probe. All samples were analyzed as replicates of four wells. Relative quantitation of the data from 7700 SDS was done using SDS 2.1 Software (Applied Biosystems).

IGF-IR activation and signaling. Cells were plated in 100-mm culture dishes and washed twice with 1× PBS before being serum starved for 14 to 16 h in modified IMEM containing 1.2 mg/mL G418 (Invitrogen). Cells were then washed once with PBS and treated for 3 min with 100 pmol/L IGF-I (a gift from Dr. J. Toretsky, Georgetown University, Washington, DC) or long-R3-IGF-I (GroPep) in IMEM at 37°C. The medium was immediately aspirated and cells were scraped from the flask and suspended in 2× cell lysis buffer (Cell Signaling) containing phosphatase inhibitors and protease inhibitors by using Complete Mini tablets (Roche). Western blot analysis was completed as described above with anti–IGF-IRβ (Cell Signaling), anti–phospho-IGF-IR (Tyr^{1131}) (Cell Signaling), anti–insulin receptor substrate 1 (IRS-1; Upstate), anti–IRS-1[pY^{612}] (Biosource), anti–phosphatidylinositol 3-kinase (PI3K) p85 (Cell Signaling), and anti–phospho-PI3K [pY^{458}] (Cell Signaling) primary antibodies. Bands were quantified by Scion Imager software and *P* values were assessed from triplicate experiments by *t* test analysis using Prism GraphPad software (*, $P < 0.05$; **, $P < 0.005$; ***, $P < 0.001$).

Cell proliferation assay. PC-3, PC-3(pcDNA3.1), and PC-3(NKX3.1) cells were seeded in triplicate in 96-well plates at a concentration of 4,000 per well in IMEM containing 10% FBS (PC-3) or 10% FBS plus 1.2 mg/mL G418 [PC-3(pcDNA3.1) and PC-3(NKX3.1)] and incubated for 24 h at 37°C. At 24, 48, 72, and 96 h after seeding, wells were trypsinized, suspended in IMEM, and immediately counted in a Beckman Coulter Z1 cell counter. Doubling times were calculated using Microsoft Excel and *P* values were calculated by ANOVA.

Tumor xenografts. Animal studies were carried out under the approved protocol AAAA-7422 as per Columbia University Institutional Animal Care and Use Committee guidelines and approval. Cell lines were grown to 80% confluence in IMEM + 10% FBS + 1.2 mg/mL G418 in a Hyperflask (Corning) and trypsinized with 0.25% trypsin-EDTA (Invitrogen). Cells were resuspended in IMEM containing 10% FBS to deactivate trypsin and washed twice with PBS. Cells were then counted and resuspended in PBS at a concentration of 3×10^7/mL. Cell suspensions (150 μL) were injected into 5-wk-old female NCr-Nude mice (Taconic Farms) on their ventral surface

Figure 1. NKX3.1 up-regulates the expression of IGFBP-3 in prostate cancer cell lines. *A,* Western blot analysis of cell extracts from stably expressing PC-3(pcDNA3.1) and PC-3(NKX3.1)-1 cell clones that have been analyzed by expression array. *B, left,* Western blot analysis of extracts from additional PC-3 clones expressing NKX3.1. *Right,* RT-PCR analysis of PC-3(pcDNA3.1) and PC-3(NKX3.1) clones for *NKX3.1* and *IGFBP-3* expression. A172 cell extract is a positive control for *IGFBP-3* expression and LNCaP cell extract is used as a positive control for *NKX3.1* expression. *C, left,* Western blot analysis of extracts from PC-3 cells transiently transfected with an NKX3.1 expression vector. *Right,* Western blot analysis of extracts from LNCaP cells transiently transfected with an NKX3.1 expression vector or serum starved in medium supplemented with 5% charcoal-stripped calf serum overnight and treated with 10 nmol/L R1881. *D,* RT-PCR analysis of *IGFBP-4* mRNA expression in PC-3(pcDNA3.1) and PC-3(NKX3.1) clones.
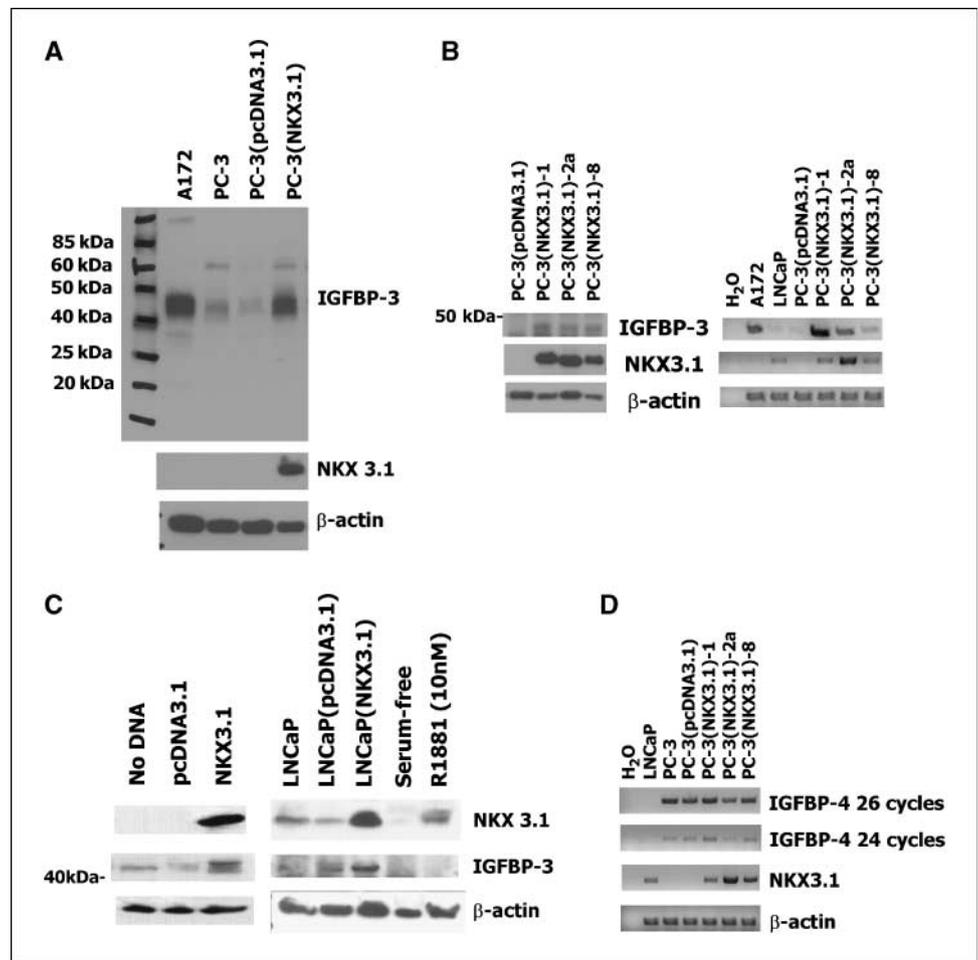
and tumors were measured in two dimensions once a week. We performed 20 inoculations per cell line. All measurements were done by one observer (E.M.). Once the tumors reached 500 mm³ or if illness was observed, mice were sacrificed and tumors were dissected and stored in 10% buffered formalin for paraffin embedding or in RNA*later* (Qiagen) at −80°C for Western blot analysis.

Immunohistochemistry. Cells grown under tissue culture conditions were embedded in 1% agarose before sectioning and staining. Paraffin embedding and sectioning of the tumor xenografts and agarose cell plugs were done by the Molecular Pathology Shared Resource of the Herbert Irving Comprehensive Cancer Center at Columbia University. Slides were microwaved for 5 min and immersed in two washes of xylene, followed by successive washes in 100%, 90%, and 70% ethanol and then by a 5-min wash in PBS. Slides were immersed in 10 mmol/L citrate buffer at pH 6.0 and steamed in a Black and Decker vegetable steamer for 40 min. Slides were fully cooled to room temperature and washed once with PBS before the blocking step, horse serum in PBS (1:66, Pierce) for 30 min at room temperature. NKX3.1 primary antibody (1:500; Zymed) was applied for 1 h at room temperature followed by biotin antimouse secondary antibody for 30 min (1:200; Vector Laboratories). This was followed by application of Vectastain Elite ABC kit (Vector Laboratories) and Vector VIP substrate kit (Vector Laboratories). Methyl green (Vector Laboratories) was used as a nuclear counterstain.

Small interfering RNA knockdown of IGFBP-3. A series of small interfering RNA (siRNA) oligonucleotides were purchased from Dharmacon. Another siRNA sequence was derived from sequences published by Stewart and colleagues (21): a siRNA duplex directed against nucleotides 603 to 623 of IGFBP-3 mRNA (reference sequence NM_000598; 5′-

AAUCAUCAUCAAGAAAGGGCA-3′). Control siRNA sequences included a mismatched oligonucleotide that differed from the IGFBP-3 siRNA oligonucleotide by 1 bp (5′-AAUCAUCUACAAGAAAGGGCA-3′), and the lamin A/C positive control sequence (5′-GGUGGUGACGAUGUGGGCU-3′). This single siRNA sequence was the only one of 11 siRNA sequences tested. The 10 *IGFBP-3* siRNA sequences that had no effect are shown in Supplementary Table S1. Cells (2×10^5) were plated in triplicate in a six-well plate in IMEM + 10% FBS + 1.2 mg/mL G418 the night before the exposure to the oligonucleotides. Cells were transfected with 20 μmol/L of siRNA oligonucleotide using Lipofectamine (Invitrogen) in Opti-MEM (Invitrogen). The medium was changed back to IMEM + 10% FBS + 1.2 mg/mL G418 at 3.5 h posttransfection, and knockdown of IGFBP-3 mRNA was assayed at 24 and 96 h by RT-PCR. In the cell proliferation assay, knockdown was allowed to proceed for 24 h before the initial cell count. For the assessment of IGF-IR activation and downstream signaling, 1×10^6 cells were plated in IMEM + 10% FBS + 1.2 mg/mL G418 the night before exposure to the oligonucleotides. Cells pretreated with oligonucleotide for up to 16 h were washed twice with PBS and serum starved for 14 to 16 h. Cells were further washed with PBS and treated with 100 pmol/L IGF-I for 3 min at 37°C.

Results

Effect of NKX3.1 on gene expression in PC-3 prostate cancer cells. To identify genes whose expression is affected by NKX3.1, we initially generated independently transfected clones of PC-3 prostate cancer cells chosen because PC-3 cells express essentially no NKX3.1 protein and express NKX3.1 mRNA at ~1/250 the level
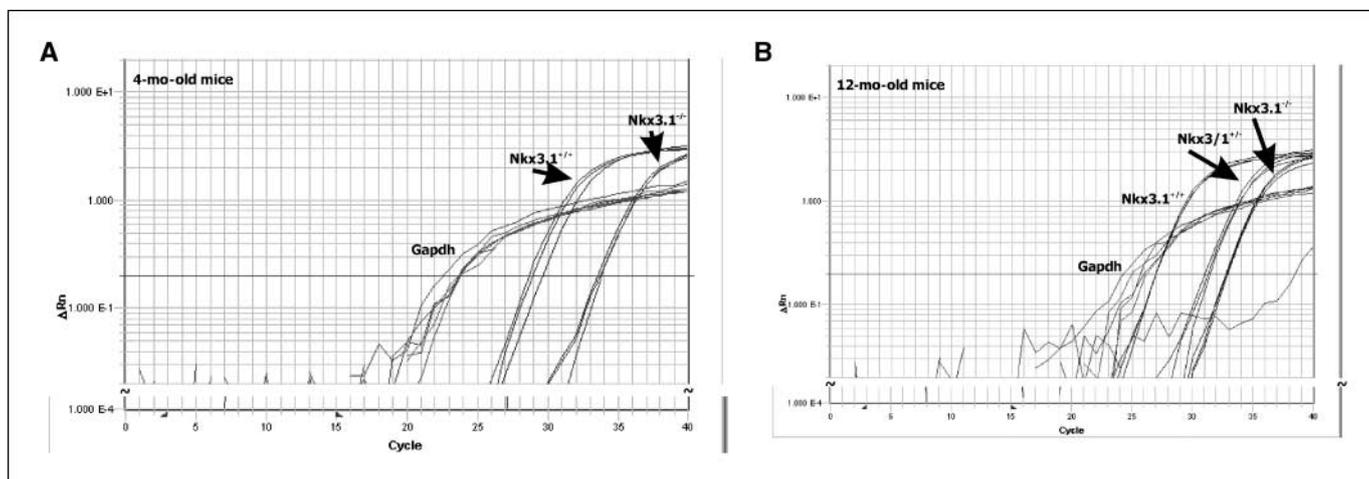
Figure 2. *Nkx3.1* and *Igfbp-3* expression in mouse prostate. Real-time RT-PCR analysis of mRNA extracts of prostatic tissue of *Nkx3.1* gene-targeted mice at 4 mo (*A*) and 12 mo (*B*) of age. Anterior prostates were analyzed from three separate animals of each genotype at each time point. *Gapdh* expression was used as a loading control. Each one of the multiple assay lines in each group represents the results of a single tissue sample. The results correlated with *Nkx3.1* genotype.

seen in LNCaP cells.[3] Two derivative PC-3 cell lines transfected with the pcDNA3.1 empty expression vector and two derivative NKX3.1 expressing clones were analyzed using the Affymetrix U-133 expression arrays. Approximately 99% of the signals obtained were regulated concordantly between the two control clones and the two NKX3.1-expressing clones. The cDNAs that were discordant between the two control clones or between the two NKX3.1-expressing clones were eliminated from the analysis, and the concordant clone expression levels were averaged across the PC-3 control cells and the PC-3(NKX3.1) cells. Then the two mean expression levels were compared. Using a cutoff of 1.4-fold up-regulation or down-regulation, 984 transcripts were identified (Supplementary Table S2). Two separate *IGFBP-3* probes were activated 9.22- and 10.23-fold in PC-3 cells expressing NKX3.1 compared with PC-3 control transfectants. The *IGFBP-3* message differences between control and NKX3.1-expressing cells were the sixth and ninth highest increases of the 508 up-regulated transcripts.

Effect of NKX3.1 on IGFBP-3 expression *in vitro*. To validate the effect of NKX3.1 on IGFBP-3 expression and determine whether protein expression was also affected, we performed Western blotting on a PC-3 clone expressing NKX3.1. NKX3.1 expression was clearly seen in transfected cells, and IGFBP-3 expression was ~10-fold activated compared with control transfected cells (Fig. 1*A*). In a separate transfection experiment, additional PC-3 clones expressing NKX3.1 were isolated. A marked increase was observed for clone 1 in Fig. 1*A*; similar but smaller increases were observed in protein and mRNA in two other clones (Fig. 1*B*).

To show that the apparent induction of IGFBP-3 expression by NKX3.1 was not an adaptation of the cells during clonal selection, we performed Western blotting on PC-3 cells transiently trans-fected with NKX3.1 and again observed increase expression of IGFBP-3 (Fig. 1*C*). The relationship between expression of NKX3.1 and expression of IGFBP-3 was not exclusive to PC-3 cells because increasing NKX3.1 expression in LNCaP cells by transfection of an NKX3.1 expression vector also increased expression of IGFBP-3

(Fig. 1*C*). Note that exposure to the synthetic androgen R1881 activated NKX3.1 expression but not IGFBP-3. This may be due to proliferative signals of R1881 that interfere with the activation of IGFBP-3 by NKX3.1. Alternatively, LNCaP cells may have down-regulated expression of IGFBP-3 as an adaptation to growth with continuous expression of NKX3.1. However, it should be noted that differences in the medium in which PC-3 and LNCaP cells were cultured may have also contributed to the differences in IGFBP-3 expression in these two cell lines. We also noted that a single probe for *IGFBP-4* was activated 4-fold by NKX3.1 in the expression array analysis. However, increased expression of *IGFBP-4* mRNA was not seen in multiple other PC-3 clones engineered to express NKX3.1 (Fig. 1*D*). LNCaP cells have been shown not to express IGFBP-4 and are used as a negative control in this Western blot, whereas PC-3 cells have been shown to express IGFBP-4 (22). No other IGF binding protein mRNAs were found to be activated in the expression array.

Expression of IGFBP-3 in prostate tissues correlates with expression of NKX3.1. To determine whether the correlation of NKX3.1 and IGFBP-3 expression could also be observed *in vivo*, we analyzed prostate mRNA in *Nkx3.1* gene-targeted mice. We have published quantitation of Nkx3.1 protein in intact, *Nkx3.1*[+/−], and *Nkx3.1*[−/−] mice, showing that levels of Nkx3.1 protein correlated with gene copy number in Nkx3.1-targeted mice (3). We performed real-time RT-PCR of RNA extracted from these mice. Data in Fig. 2 show that *Igfbp-3* mRNA expression was related to *Nkx3.1* gene copy number in murine prostates. In each reaction, *Gapdh* was used as a control and was invariant between the different strains. We found that in murine prostates, *Igfbp-3* expression levels correlated with *Nkx3.1* copy number and thus with *Nkx3.1* expression (Fig. 2).

Although we had shown an increase in *IGFBP-3* mRNA as a result of NKX3.1 expression in cultured human cells, we were unable to show an effect of NKX3.1 on luciferase reporter constructs that contained regions from the *IGFBP-3* gene promoter (data not shown; ref. 23). This is not entirely surprising because NKX3.1 by itself does not contribute to the formation of a transcriptional complex and suppresses transcription from reporter constructs engineered with the NKX3.1 cognate DNA binding domain (19).

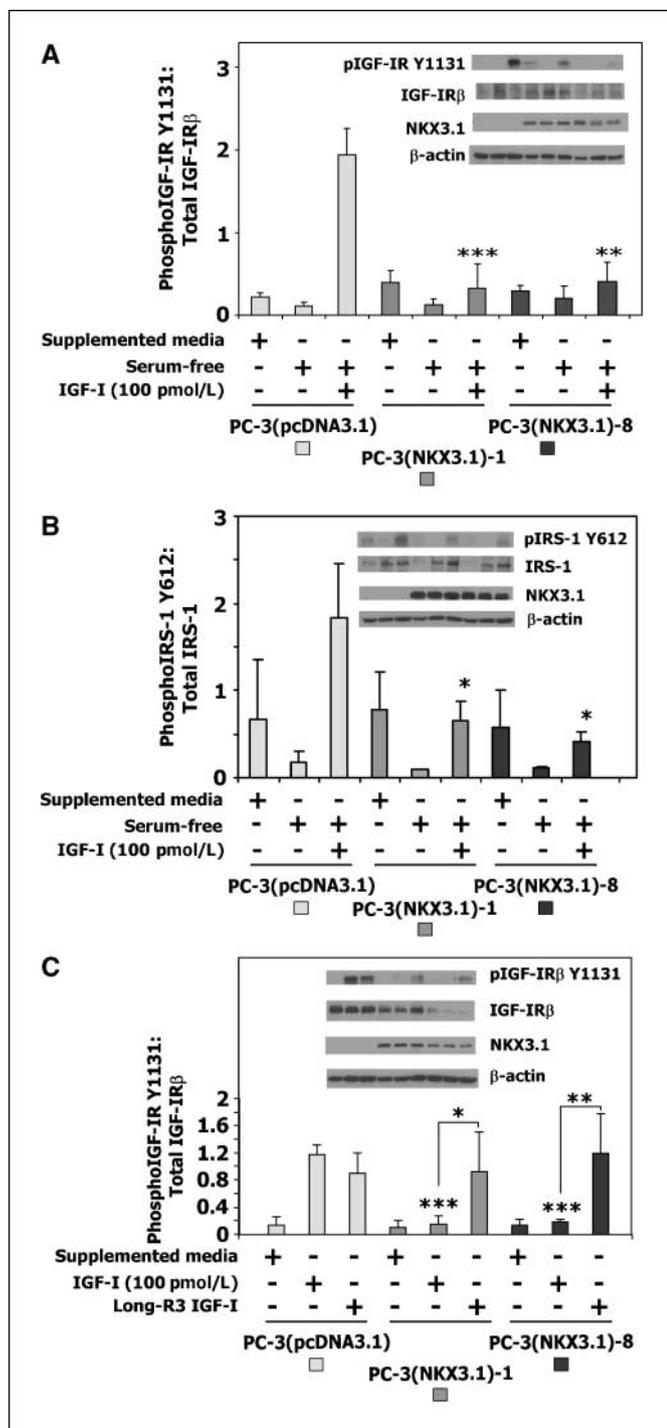---

[3] Our unpublished data.

Figure 3. NKX3.1 expression inhibits the IGF-1–mediated phosphorylation of the IGF-1R and IRS-1 in PC-3 cells. A, Western blot analysis of extracts from PC-3(pcDNA3.1), PC-3(NKX3.1)-1, and PC-3(NKX3.1)-8 stable cell clones serum starved for 16 h and treated with 100 pmol/L IGF-I. The histogram of IGF-IR activation is based on three separate experiments. B, Western blot analysis of extracts from PC-3(pcDNA3.1), PC-3(NKX3.1)-1, and PC-3(NKX3.1)-8 clones serum starved for 16 h and treated with 100 pmol/L IGF-I. The histogram of IRS-1 activation is based on three separate experiments. C, Western blot analysis of extracts from PC-3(pcDNA3.1), PC-3(NKX3.1)-1, and PC-3(NKX3.1)-8 clones serum starved for 16 h and treated with 100 pmol/L IGF-1 or long-R3-IGF-I. The histogram of IGF-IR activation is based on three separate experiments. Statistical comparisons are indicated by asterisks as explained in Materials and Methods. Comparisons are versus PC-3(pcDNA3.1) treated with IGF-I unless otherwise indicated by brackets.
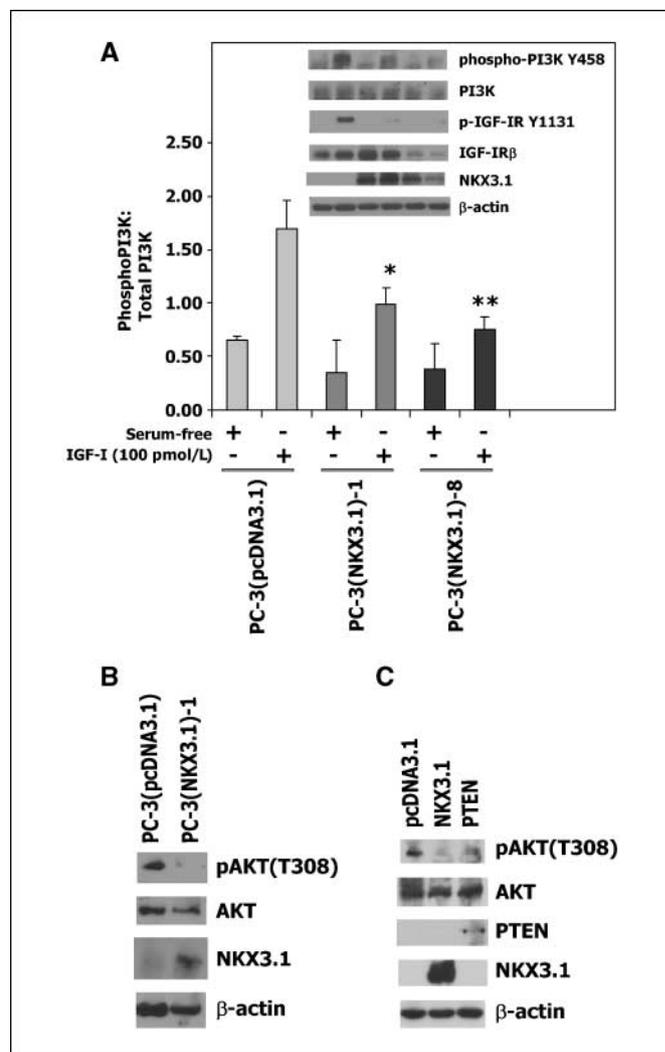

Figure 4. NKX3.1 attenuates IGF-1R downstream signaling. A, Western blot analysis of extracts from PC-3(pcDNA3.1), PC-3(NKX3.1)-1, and PC-3(NKX3.1)-8 clones serum starved for 16 h and treated with 100 pmol/L IGF-I for 3 min. The histogram of PI-3K activation is based on three separate experiments. Statistical comparisons are indicated by asterisks. Comparisons are versus PC-3(pcDNA3.1) treated with IGF-I. B, Western blot analysis of cell extracts from PC-3(pcDNA3.1) and PC-3(NKX3.1)-1 cells grown in medium containing 10% FBS. C, Western blot analysis of cell extracts of PC-3 cells transiently transfected with either a NKX3.1 or a PTEN expression vector.

The effect of NKX3.1 on IGF-I signaling. To determine whether the induction of IGFBP-3 expression by NKX3.1 affected IGF-I signaling, we examined the response of the IGF-IR to IGF-I in derivative PC-3 cells. In the presence of serum-free medium, IGF-I induced IGF-IR phosphorylation at Tyr[1131] within 3 minutes of exposure to the ligand (24). Phosphorylation of IGF-IR was diminished in cells expressing NKX3.1 (Fig. 3A). The effect of NKX3.1 on IGF-IR activation could also be seen on downstream signaling targets. IGF-I–induced phosphorylation of IRS-1, a target of both the insulin receptor and IGF-IR, was diminished in cells expressing NKX3.1 (Fig. 3B). PC-3 derivative cells were also treated with the long-R3-IGF-I that has minimal binding to IGFBP-3 (25, 26). Long-R3-IGF-I activated phosphorylation of IGF-IR equally well in derivative PC-3 cells regardless of NKX3.1 expression (Fig. 3C). This result is consistent with the notion that NKX3.1 mediates inhibition of IGF-I signaling via increased expression of IGFBP-3.

We examined the effect of NKX3.1 expression on the phosphorylation of PI3K and its downstream target AKT. PI3K phosphorylation was diminished to some degree by expression of NKX3.1 in two PC-3(NKX3.1) clones (Fig. 4A). AKT phosphorylation was also decreased in a PC-3(NKX3.1) clone grown in serum-supplemented medium that contains IGF-I from FBS (Fig. 4B). We compared the effects of NKX3.1 expression and PTEN expression in transient transfection of PC-3 cells and saw comparable degrees of reduction in p-AKT (Fig. 4C).

Growth suppression by NKX3.1 is mediated by IGFBP-3. *In vitro* growth of the parental and derivative PC-3 cells was assessed by cell counting over 96 hours. As shown in the top section of Table 1, NKX3.1 expression decreased cell proliferation in three independent clones. The doubling times for PC-3 cells expressing NKX3.1 ranged from 25% to 60% above the doubling times for control cells. To determine whether this effect of NKX3.1 expression on cell proliferation was due to IGFBP-3 expression, we performed growth experiments in the presence of a siRNA oligonucleotide and control oligonucleotides for IGFBP-3 knockdown (21). *IGFBP-3* siRNA treatment decreased IGFBP-3 expression at both 24 and 96 hours after cells were exposed to the oligonucleotide (Fig. 5A). Growth curves of control and NKX3.1-expressing PC-3 cells were done in the presence of transfection reagent, missense oligonucleotide, and *IGFBP-3* siRNA. Only the *IGFBP-3* siRNA restored PC-3 proliferative rate to the level of the controls (Table 1, *bottom section*). Thus, IGFBP-3 mediates, at least in part, *in vitro* growth suppression by NKX3.1. Consistent with this finding, the IGFBP-3 siRNA reversed the suppression of IGF-IR phosphorylation induced by NKX3.1 (Fig. 5B). IGFBP-3 knockdown was accomplished with a single IGFBP-3 siRNA oligonucleotide as described in Materials and Methods. Of the 11 sequences tested, only one induced substantial IGFBP-3 knockdown. This one effective siRNA sequence has no identifiable homology with sequences in other genes, as confirmed by a BLAST search against the entire human genome sequence.

We also performed xenograft experiments wherein PC-3(NKX3.1) clones 1, 2, and 8 and PC-3(cDNA3.1) cells were inoculated into female *NCr/nu* mice. In every instance, we observed tumor growth of derivative PC-3 cells (Supplementary Fig. S1). Each tumor type had lost expression *in vivo* of the NKX3.1 transgene as shown by immunohistochemical analysis. Thus, there was a selection in xenografts for loss of NKX3.1 expression, preventing us from observing any growth-suppressive effects of NKX3.1 on PC-3 cells *in vivo*.

Discussion

NKX3.1 is important for prostate epithelial cell development, growth control, and differentiation (6, 27). Murine *Nkx3.1* is haploinsufficient and loss of a single allele manifests a phenotype similar to homozygous deletion, but with longer latency (6). In early human prostate cancer, we have found that NKX3.1 expression is down-regulated over a broad range, suggesting a complex effect on the development of human prostate cancer (3). It is important to define the pathways of tumorigenesis that are affected by NKX3.1. We argue here that expression of IGFBP-3 is downstream of NKX3.1 and speculate that IGFBP-3 regulates IGF-I action in prostate epithelial cells.

IGFs are peptide growth factors that bind to the IGF-IR to regulate cell growth, differentiation, and apoptosis (12). IGFs are present in abundance in the circulation and may exert systemic and local effects on cells. Circulating IGF-I is bound mainly to IGFBP-3, one of the most abundant serum proteins (28). Although IGFBP-3 can inhibit the interaction of IGF-I with its receptor at the cellular level, serum IGFBP-3 serves to stabilize circulating IGF-I (29). Serum levels of both proteins vary with age, nutrition, and hormonal status (30). The interaction of serum IGF-I and IGFBP-3 and prostate cancer risk has been studied by a number of investigators (29). The majority of studies have found an association between higher IGF-I levels and prostate cancer

Table 1. Effect of IGFBP-3 knockdown on cell proliferation

Cell line	Treatment	Doubling time (h)	*P*
PC-3	None	25.34 ± 1.91	NS
PC-3(pcDNA3.1)	None	24.26 ± 2.05	Reference
PC-3(NKX3.1)-1	None	32.24 ± 5.91	0.0037
PC-3(NKX3.1)-2a	None	38.88 ± 7.82	0.0002
PC-3(NKX3.1)-8	None	30.24 ± 2.55	0.002
PC-3(pcDNA3.1)	None	23.6 ± 2.52	Reference
PC-3(pcDNA3.1)	Mock	25.5 ± 1.23	NS
PC-3(pcDNA3.1)	Missense oligo	24.4 ± 1.86	NS
PC-3(pcDNA3.1)	IGFBP-3 siRNA oligo	26.4 ± 1.40	NS
PC-3(NKX3.1)-1	None	32.9 ± 1.33	0.0092
PC-3(NKX3.1)-1	Mock	31.7 ± 2.49	0.0013
PC-3(NKX3.1)-1	Missense oligo	32.0 ± 3.12	0.0022
PC-3(NKX3.1)-1	IGFBP-3 siRNA oligo	24.9 ± 2.56	NS

NOTE: The cell doubling time, in hours, of parental PC-3 cells, PC-3(pcDNA3.1) cells, and PC-3(NKX3.1) clones was assayed by cell counting. Cells were counted at 24, 48, 72, and 96 h after seeding and doubling times were calculated. In the bottom section of the table, PC-3(pcDNA3.1) and PC-3(NKX3.1)-1 cells were treated with transfection reagent alone, the missense siRNA oligonucleotide, and the IGFBP-3 siRNA oligonucleotide for 24 h before the first cell count was taken. *P* values were calculated in comparison with the PC-3(pcDNA3.1) cell doubling time, using ANOVA.
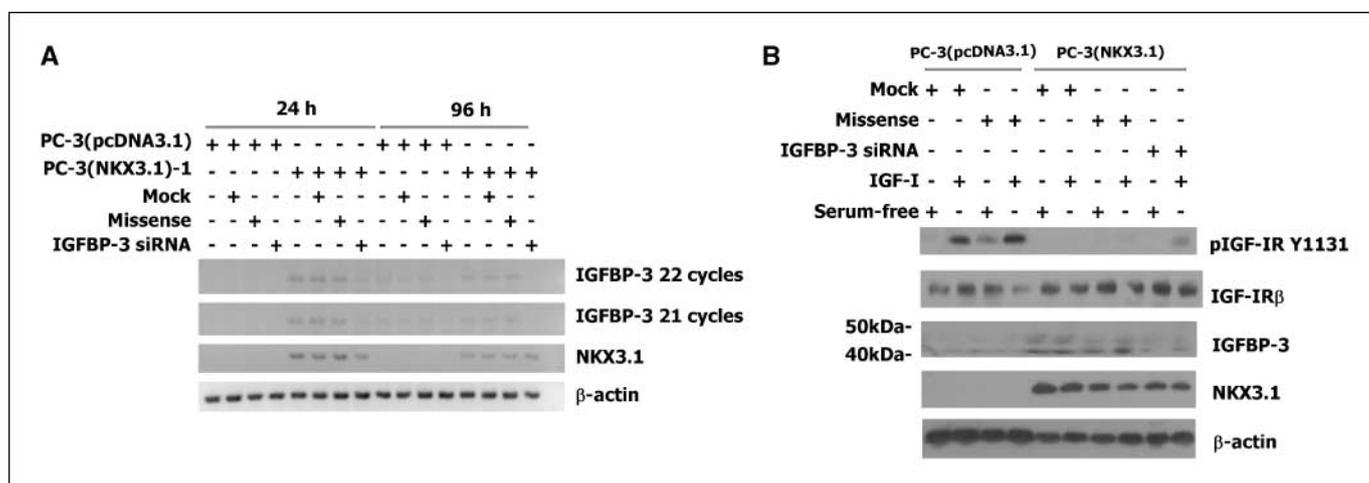Abbreviation: NS, not significant ($P > 0.05$).

Figure 5. IGFBP-3 knockdown in PC-3(NKX3.1) cells. *A,* RT-PCR analysis of mRNA from PC-3(pcDNA3.1) and PC-3(NKX3.1)-1 cells that were treated with transfection reagent alone, missense oligo, or the IGFBP-3 siRNA oligo at 24 and 96 h posttransfection. *B,* Western blot analysis of extracts from PC-3(pcDNA3.1) and PC-3(NKX3.1)-1 cells treated with transfection reagent alone, missense oligo, or the IGFBP-3 siRNA oligo for 96 h, which afterward were serum starved for 16 h and treated with 100 pmol/L IGF-I.

(31–39). Some investigators have not been able to confirm these findings (40–42).

NKX3.1 haploinsufficiency affects cell transformation, at least in part, by downstream effects on transcriptional targets. NKX3.1 binds to DNA and suppresses expression of genes downstream from cognate DNA binding sites (19). We have yet to identify a promoter that is transcriptionally activated by direct binding of NXK3.1 to its cognate DNA -TAAGTA- sequence. In fact, our experiments with reporter constructs containing NKX3.1 binding DNA suggested that NKX3.1 alone cannot initiate assembly of a transcriptional complex (19). NKX3.1 is known to interact with other transcription factors such as serum response factor and serves as a synergistic coactivator of promoters with serum response elements such as smooth muscle γ-actin (43). Therefore, the effect of NKX3.1 on gene expression is complex and is likely mediated by a number of cofactors. Because other NK homeodomain protein family members like Nkx2.5 interact with serum response factor, the physical interaction of NKX3.1 and serum response factor has been studied as a model for transcription factor interactions of NKX3.1. Serum response factor is a widely expressed transcription factor involved in orchestrating disparate programs of gene expression linked to muscle differentiation and cellular growth (44). It is likely that different targets of transcriptional activation are affected by the interaction of NKX3.1 with several different transcription factors.

We have shown an indirect link between NKX3.1 and transcription of IGFBP-3 mRNA. In cultured cells with NKX3.1 overexpression, we have shown a mechanistic link between NKX3.1, IGFBP-3 expression, IGF-IR activation, and cell proliferation. IGF1-R signaling is complex and affected by many factors that regulate IGF-I availability and intracellular signaling downstream from the IGF-IR. Therefore, the interaction between NKX3.1 and IGFBP-3 expression *in vivo* is likely to be part of a more complex system regulating the effect of IGF-I on prostate epithelial cells. The IGFBPs have functions that can compensate for one another, making it difficult to determine specific functions of a single IGF

binding protein by studies of gene-targeted mice (45, 46). Whether the same compensatory activation of IGF binding proteins occurs in prostate epithelial cells that have reduced NKX3.1 expression was not determined.

Down-regulation of NKX3.1 protein per se is sufficient to predispose cells to malignant transformation. In addition, we have described a family in which hereditary prostate cancer cosegregated with a T164A missense mutation in the NKX3.1 homeodomain that reduced DNA binding by 95% (47). Haploinsufficiency is a reflection of the dominant nature of regulation by NK family members. Both missense and truncation mutations in NKX2.5 are autosomal dominant determinants of congenital cardiac abnormalities (48, 49). Similarly, mutations in NKX2.1/TTF cause pulmonary and thyroid developmental abnormalities (50). Paradoxically, *NKX2.1* is amplified in a subset of lung cancers and NKX2.1 overexpression contributes to cell transformation and oncogenesis (51). We argue that tumor suppression by NKX3.1 is exerted in a relative manner by modulation of downstream targets to different degrees. Our finding that IGFBP-3 expression in human prostate cancer cells correlates quantitatively with NKX3.1 expression levels is reminiscent of findings that *Nkx3.1* gene dosage determines the degree of transcriptional effects in gene-targeted mice (8). Further studies will identify additional NKX3.1 targets and elucidate their role in prostate cancer suppression and, perhaps, prevention.

Disclosure of Potential Conflicts of Interest

No potential conflicts of interest were disclosed.

Acknowledgments

References

1. Swalwell JI, Vocke CD, Yang Y, et al. Determination of a minimal deletion interval on chromosome band 8p21 in sporadic prostate cancer. Genes Chromosomes Cancer 2002;33:201–5.

2. Bowen C, Bubendorf L, Voeller HJ, et al. Loss of NKX3.1 expression in human prostate cancers correlates with tumor progression. Cancer Res 2000;60:6111–5.

3. Asatiani E, Huang WX, Wang A, et al. Deletion, methylation, and expression of the NKX3.1 suppressor gene in primary human prostate cancer. Cancer Res 2005;65:1164–73.

4. Voeller HJ, Augustus M, Madlike V, et al. Coding region of NKX3.1, prostate-specific homeobox gene on 8p21, is not mutated in human prostate cancers. Cancer Res 1997;57:4455–9.

5. Ornstein DK, Cinquanta M, Weiler S, et al. Expression studies and mutational analysis of the androgen regulated homeobox gene nkx3.1 in benign and malignant prostate epithelium. J Urol 2001;165:1329–34.

6. Bhatia-Gaur R, Donjacour AA, Sciavolino PJ, et al. Roles for Nkx3.1 in prostate development and cancer. Genes Dev 1999;13:966–77.

7. Kim MJ, Cardiff RD, Desai N, et al. Cooperativity of Nkx3.1 and Pten loss of function in a mouse model of prostate carcinogenesis. Proc Natl Acad Sci U S A 2002; 99:2884–9.

8. Magee JA, Abdulkadir SA, Milbrandt J. Haploinsufficiency at the Nkx3.1 locus. A paradigm for stochastic, dosage-sensitive gene regulation during tumor initiation. Cancer Cell 2003;3:273–83.

9. Bethel CR, Faith D, Li X, et al. Decreased NKX3.1 protein expression in focal prostatic atrophy, prostatic intraepithelial neoplasia, and adenocarcinoma: association with gleason score and chromosome 8p deletion. Cancer Res 2006;66:10683–90.

10. Markowski MC, Bowen C, Gelmann EP. Inflammatory cytokines induce phosphorylation and ubiquitination of prostate suppressor protein NKX3.1. Cancer Res 2008; 68:6896–901.

11. Firth SM, Baxter RC. Cellular actions of the insulin-like growth factor binding proteins. Endocr Rev 2002;23: 824–54.

12. Khandwala HM, McCutcheon IE, Flyvbjerg A, Friend KE. The effects of insulin-like growth factors on tumorigenesis and neoplastic growth. Endocr Rev 2000;21:215–44.

13. Cohen P, Graves HC, Peehl DM, et al. Prostate-specific antigen (PSA) is an insulin-like growth factor binding protein-3 protease found in seminal plasma. J Clin Endocrinol Metab 1992;75:1046–53.

14. Koistinen H, Paju A, Koistinen R, et al. Prostate-specific antigen and other prostate-derived proteases cleave IGFBP-3, but prostate cancer is not associated with proteolytically cleaved circulating IGFBP-3. Prostate 2002;50:112–8.

15. Fielder PJ, Rosenfeld RG, Graves HC, et al. Biochemical analysis of prostate specific antigen-proteolyzed insulin-like growth factor binding protein-3. Growth Regul 1994;4:164–72.

16. Cohen P, Peehl DM, Graves HC, Rosenfeld RG. Biological effects of prostate specific antigen as an insulin-like growth factor binding protein-3 protease. J Endocrinol 1994;142:407–15.

17. Hong J, Zhang G, Dong F, Rechler MM. Insulin-like growth factor (IGF)-binding protein-3 mutants that do not bind IGF-I or IGF-II stimulate apoptosis in human prostate cancer cells. J Biol Chem 2002;277:10489–97.

18. Rhodes DR, Barrette TR, Rubin MA, Ghosh D, Chinnaiyan AM. Meta-analysis of microarrays: inter-study validation of gene expression profiles reveals pathway dysregulation in prostate cancer. Cancer Res 2002;62:4427–33.

19. Steadman DJ, Giuffrida D, Gelmann EP. DNA-binding sequence of the human prostate-specific homeodomain protein NKX3.1. Nucleic Acids Res 2000;28:2389–95.

20. Wu X, Senechal K, Neshat MS, Whang YE, Sawyers CL. The PTEN/MMAC1 tumor suppressor phosphatase functions as a negative regulator of the phosphoinositide 3-kinase/Akt pathway. Proc Natl Acad Sci U S A 1998;95:15587–91.

21. Stewart LV, Weigel NL. Role of insulin-like growth factor binding proteins in 1α,25-dihydroxyvitamin D₃-induced growth inhibition of human prostate cancer cells. Prostate 2005;64:9–19.

22. Kimura G, Kasuya J, Giannini S, et al. Insulin-like growth factor (IGF) system components in human prostatic cancer cell-lines: LNCaP, DU145, and PC-3 cells. Int J Urol 1996;3:39–46.

23. Walker GE, Wilson EM, Powell D, Oh Y. Butyrate, a histone deacetylase inhibitor, activates the human IGF binding protein-3 promoter in breast cancer cells: molecular mechanism involves an Sp1/Sp3 multiprotein complex. Endocrinology 2001;142:3817–27.

24. Hernandez-Sanchez C, Blakesley V, Kalebic T, Helman L, LeRoith D. The role of the tyrosine kinase domain of the insulin-like growth factor-I receptor in intracellular signaling, cellular proliferation, and tumorigenesis. J Biol Chem 1995;270:29176–81.

25. Francis GL, Ross M, Ballard FJ, et al. Novel recombinant fusion protein analogues of insulin-like growth factor (IGF)-I indicate the relative importance of IGF-binding protein and receptor binding for enhanced biological potency. J Mol Endocrinol 1992;8:213–23.

26. King R, Wells JR, Krieg P, et al. Production and characterization of recombinant insulin-like growth factor-I (IGF-I) and potent analogues of IGF-I, with Gly or Arg substituted for Glu3, following their expression in *Escherichia coli* as fusion proteins. J Mol Endocrinol 1992;8:29–41.

27. Abdulkadir SA, Magee JA, Peters TJ, et al. Conditional loss of Nkx3.1 in adult mice induces prostatic intraepithelial neoplasia. Mol Cell Biol 2002;22:1495–503.

28. Jones JI, Clemmons DR. Insulin-like growth factors and their binding proteins: biological actions. Endocr Rev 1995;16:3–34.

29. Pollak MN, Schernhammer ES, Hankinson SE. Insulin-like growth factors and neoplasia. Nat Rev Cancer 2004;4:505–18.

30. Rajaram S, Baylink DJ, Mohan S. Insulin-like growth factor-binding proteins in serum and other biological fluids: regulation and functions. Endocr Rev 1997;18: 801–31.

31. Harman SM, Metter EJ, Blackman MR, Landis PK, Carter HB. Serum levels of insulin-like growth factor I (IGF-I), IGF-II, IGF-binding protein-3, and prostate-specific antigen as predictors of clinical prostate cancer. J Clin Endocrinol Metab 2000;85:4258–65.

32. Chan JM, Stampfer MJ, Ma J, et al. Insulin-like growth factor-I (IGF-I) and IGF binding protein-3 as predictors of advanced-stage prostate cancer. J Natl Cancer Inst 2002;94:1099–106.

33. Chokkalingam AP, Pollak M, Fillmore CM, et al. Insulin-like growth factors and prostate cancer: a population-based case-control study in China. Cancer Epidemiol Biomarkers Prev 2001;10:421–7.

34. Oliver SE, Gunnell D, Donovan J, et al. Screen-detected prostate cancer and the insulin-like growth factor axis: results of a population-based case-control study. Int J Cancer 2004;108:887–92.

35. Platz EA, Pollak MN, Leitzmann MF, et al. Plasma insulin-like growth factor-1 and binding protein-3 and subsequent risk of prostate cancer in the PSA era. Cancer Causes Control 2005;16:255–62.

36. Stattin P, Bylund A, Rinaldi S, et al. Plasma insulin-like growth factor-I, insulin-like growth factor-binding proteins, and prostate cancer risk: a prospective study. J Natl Cancer Inst 2000;92:1910–7.

37. Stattin P, Rinaldi S, Biessy C, et al. High levels of circulating insulin-like growth factor-I increase prostate cancer risk: a prospective study in a population-based nonscreened cohort. J Clin Oncol 2004;22:3104–12.

38. Li L, Yu H, Schumacher F, Casey G, Witte JS. Relation of serum insulin-like growth factor-I (IGF-I) and IGF binding protein-3 to risk of prostate cancer (United States). Cancer Causes Control 2003;14:721–6.

39. Wolk A, Mantzoros CS, Andersson SO, et al. Insulin-like growth factor 1 and prostate cancer risk: a population-based, case-control study. J Natl Cancer Inst 1998;90:911–5.

40. Janssen JA, Wildhagen MF, Ito K, et al. Circulating free insulin-like growth factor (IGF)-I, total IGF-I, and IGF binding protein-3 levels do not predict the future risk to develop prostate cancer: results of a case-control study involving 201 patients within a population-based screening with a 4-year interval. J Clin Endocrinol Metab 2004;89:4391–6.

41. Woodson K, Tangrea JA, Pollak M, et al. Serum insulin-like growth factor I: tumor marker or etiologic factor? A prospective study of prostate cancer among Finnish men. Cancer Res 2003;63:3991–4.

42. Chen C, Lewis SK, Voigt L, et al. Prostate carcinoma incidence in relation to prediagnostic circulating levels of insulin-like growth factor I, insulin-like growth factor binding protein 3, and insulin. Cancer 2005;103:76–84.

43. Carson JA, Fillmore RA, Schwartz RJ, Zimmer WE. The smooth muscle γ-actin gene promoter is a molecular target for the mouse bagpipe homologue, mNkx3-1, and serum response factor. J Biol Chem 2000; 275:39061–72.

44. Miano JM. Serum response factor: toggling between disparate programs of gene expression. J Mol Cell Cardiol 2003;35:577–93.

45. Ning Y, Schuller AG, Bradshaw S, et al. Diminished growth and enhanced glucose metabolism in triple knockout mice containing mutations of insulin-like growth factor binding protein-3, -4, and -5. Mol Endocrinol 2006;20:2173–86.

46. Wood TL, Rogler LE, Czick ME, Schuller AGP, Pintar JE. Selective alterations in organ sizes in mice with a targeted disruption of the insulin-like growth factor binding protein-2 gene. Mol Endocrinol 2000;14: 1472–82.

47. Zheng SL, Ju JH, Chang BL, et al. Germ-line mutation of NKX3.1 cosegregates with hereditary prostate cancer and alters the homeodomain structure and function. Cancer Res 2006;66:69–77.

48. Benson DW, Silberbach GM, Kavanaugh-McHugh A, et al. Mutations in the cardiac transcription factor NKX2.5 affect diverse cardiac developmental pathways. J Clin Invest 1999;104:1567–73.

49. Kasahara H, Lee B, Schott JJ, et al. Loss of function and inhibitory effects of human CSX/NKX2.5 homeoprotein mutations associated with congenital heart disease. J Clin Invest 2000;106:299–308.

50. Iwatani N, Mabe H, Devriendt K, Kodama M, Miike T. Deletion of NKX2.1 gene encoding thyroid transcription factor-1 in two siblings with hypothyroidism and respiratory failure. J Pediatr 2000;137:272–6.

51. Weir BA, Woo MS, Getz G, et al. Characterizing the cancer genome in lung adenocarcinoma. Nature 2007; 450:893–8.

AACR American Association for Cancer Research

Cancer Research

NKX3.1 Activates Expression of Insulin-like Growth Factor Binding Protein-3 to Mediate Insulin-like Growth Factor-I Signaling and Cell Proliferation

Erin Muhlbradt, Ekaterina Asatiani, Elizabeth Ortner, et al.

Updated version	Access the most recent version of this article at: doi:10.1158/0008-5472.CAN-08-3022
Supplementary Material	Access the most recent supplemental material at: http://cancerres.aacrjournals.org/content/suppl/2009/02/23/0008-5472.CAN-08-3022.DC1

Cited articles	This article cites 51 articles, 20 of which you can access for free at: http://cancerres.aacrjournals.org/content/69/6/2615.full#ref-list-1
Citing articles	This article has been cited by 4 HighWire-hosted articles. Access the articles at: http://cancerres.aacrjournals.org/content/69/6/2615.full#related-urls

E-mail alerts	Sign up to receive free email-alerts related to this article or journal.
Reprints and Subscriptions	To order reprints of this article or to subscribe to the journal, contact the AACR Publications Department at pubs@aacr.org.
Permissions	To request permission to re-use all or part of this article, use this link http://cancerres.aacrjournals.org/content/69/6/2615. Click on "Request Permissions" which will take you to the Copyright Clearance Center's (CCC) Rightslink site.